

Supporting Information

Highly stretchable, adhesive and 3D-printable eutectic ion conductor for wearable electronics and self-powered sensors

Xiaohu Li,¹ Xuhang Zhang,¹ Zhisen Zhu,² Wenling Zhang² and Yingdan Liu^{1*}

¹Center for Advanced Structural Materials, State Key Lab of Metastable Materials Science and Technology, and College of Materials Science and Engineering, Yanshan University, Qinhuangdao 066004, P.R. China

E-mail: ydliu@ysu.edu.cn

²School of Mechanical Engineering, Nanjing University of Science and Technology, Nanjing 210094, China

Contents

Section S1 Supplementary Tables

Section S2 Supplementary Figures

Section S3 Supplementary Movie

Section S1 Supplementary Tables

Table S1. The compositions of EICs with various x (y=2).

Sample	LiTFSI (g)	AAm (g)	EG (g)	AMCO (g)	PEGDA400 (μ L)	TPO (mg)
AMMO ₀₋₂	3.15	1.56	2.72	0	2.8	3.1
AMMO _{0.5-2}	2.87	1.42	2.48	1.41	5.0	5.7
AMMO ₁₋₂	3.15	1.56	2.72	3.10	8.3	9.3
AMMO _{1.25-2}	3.15	1.56	2.72	3.87	9.7	10.9
AMMO _{1.5-2}	3.15	1.56	2.72	4.65	11.1	12.4

Table S2. The compositions of EICs with various x (y=2). The fixed amount of PEGDA was 9.7 μ L.

Sample	LiTFSI (g)	AAm (g)	EG (g)	AMCO (g)	PEGDA400 (μ L)	TPO (mg)
AMMO ₀₋₂	3.15	1.56	2.72	0	9.7	3.1
AMMO ₁₋₂	3.15	1.56	2.72	3.10	9.7	9.3
AMMO _{1.25-2}	3.15	1.56	2.72	3.87	9.7	10.9
AMMO _{1.25-2}	3.15	1.56	2.72	4.65	9.7	12.4

Table S3. The compositions of EICs with various y (x=1.25).

Sample	LiTFSI (g)	AAm (g)	EG (g)	AMCO (g)	PEGDA400 (μ L)	TPO (mg)
AMMO _{1.25-1.5}	3.15	1.56	2.04	3.87	9.7	10.9
AMMO _{1.25-2}	3.15	1.56	2.72	3.87	9.7	10.9
AMMO _{1.25-2.5}	3.15	1.56	3.40	3.87	9.7	10.9
AMMO _{1.25-3}	3.15	1.56	4.09	3.87	9.7	10.9

Section S2 Supplementary Figures

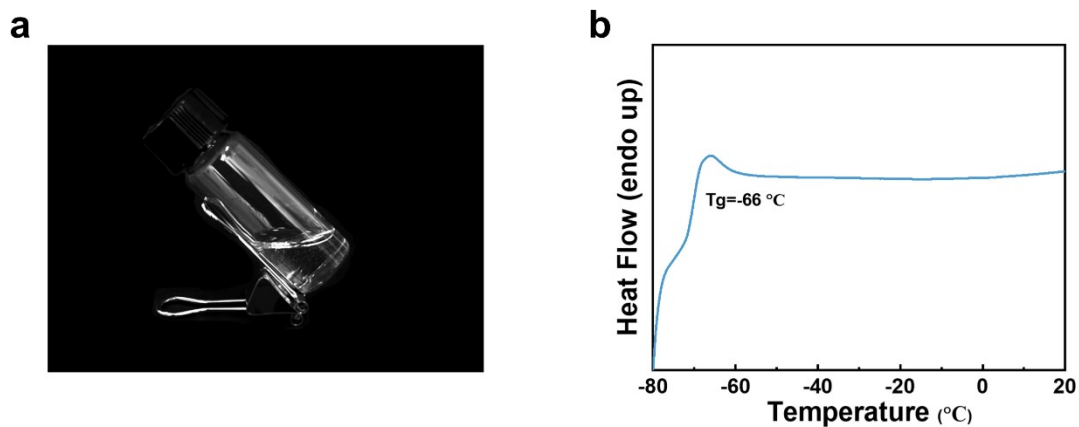


Figure S1. a) Photo of prepared ES, b) differential scanning calorimetry curves of ES.

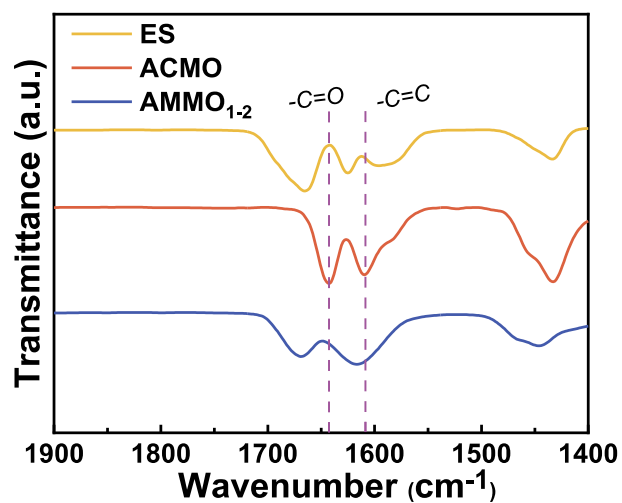


Figure S2. FT-IR spectra of ES, ACMO, AMMO₁₋₂.

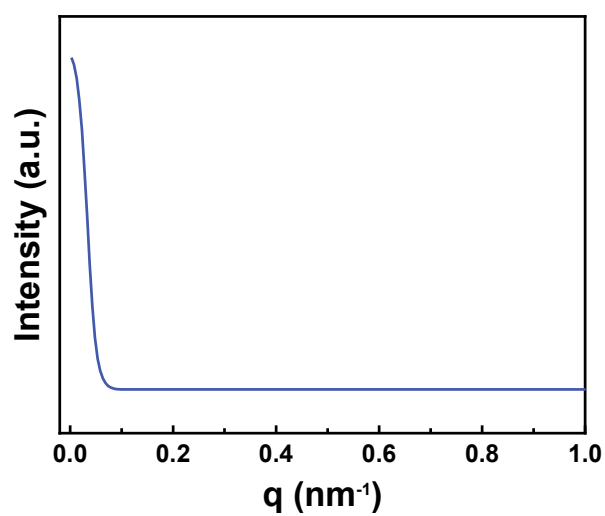


Figure S3. 1D-SAXS profile of AMMO_{1.25-2}.

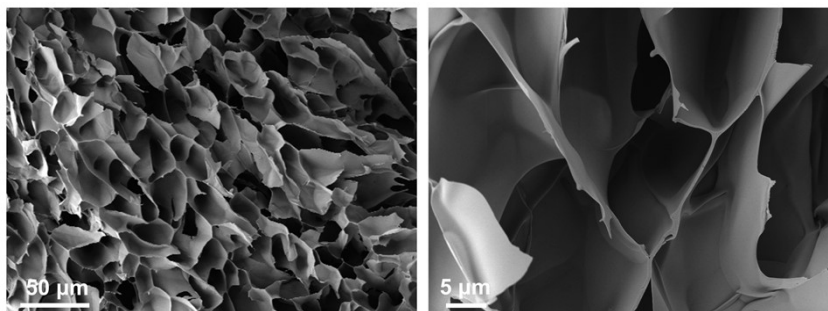


Figure S4. SEM of AMMO_{1.25-2} with water removed.

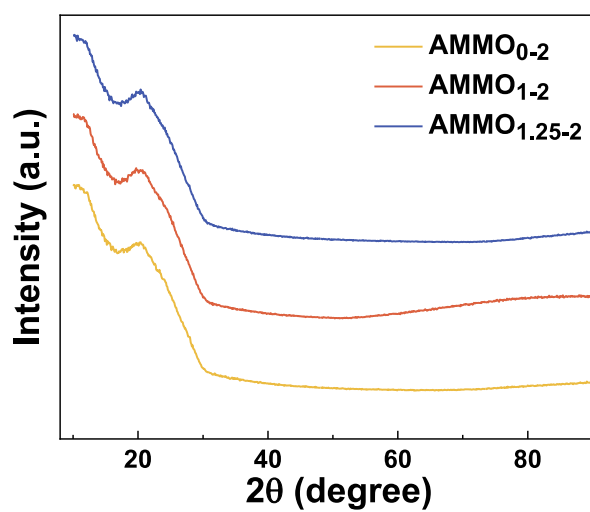


Figure S5. X-ray diffraction patterns of AMMO_{x-2}.

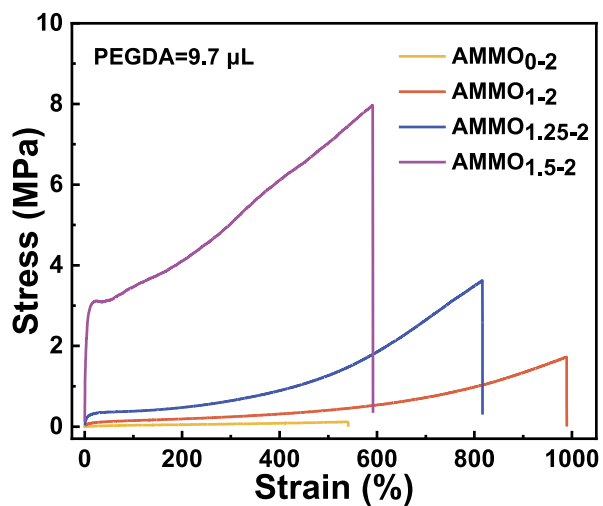


Figure S6. Stress-strain curves for EICs with varying ACMO contents. The amount of fixed PEGDA was 9.7 μ L.

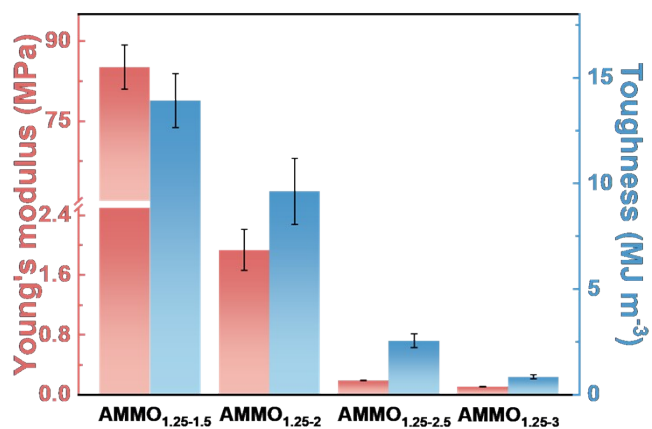


Figure S7. Stress-strain curves of AAMMO_{1.25-y} with different EG contents, (b) and their Young's modulus and toughness.

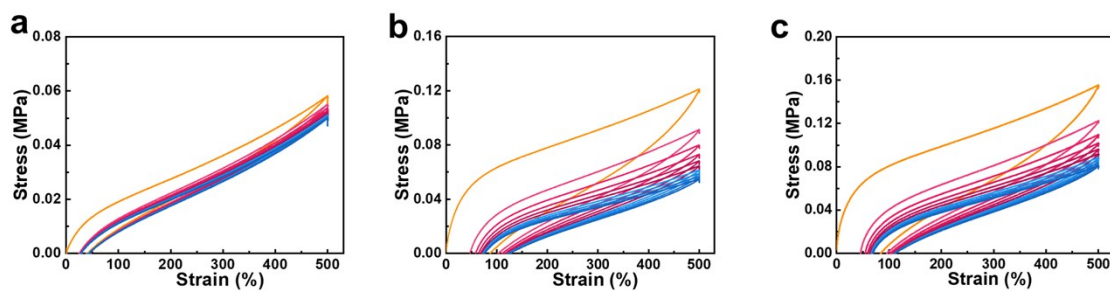


Figure S8. Cyclic loading-unloading curves of a)AMMO₀₋₂, b)AMMO₁₋₂ and c)AMMO_{1.25-2}.

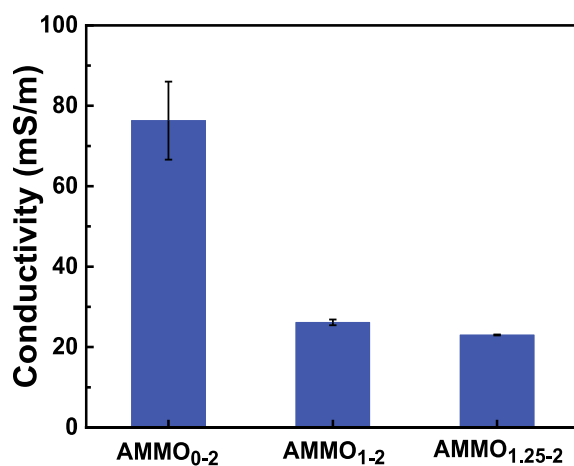


Figure S9. The conductivity of the EICs.

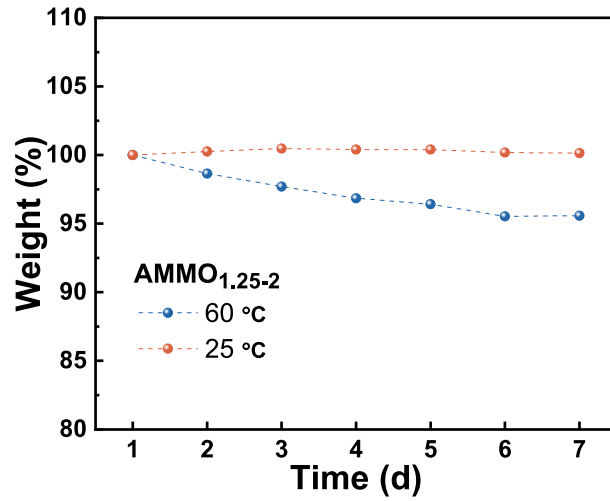


Figure S10. Mass change of AMMO_{1.25-2} in 7 days when exposed to different temperatures.

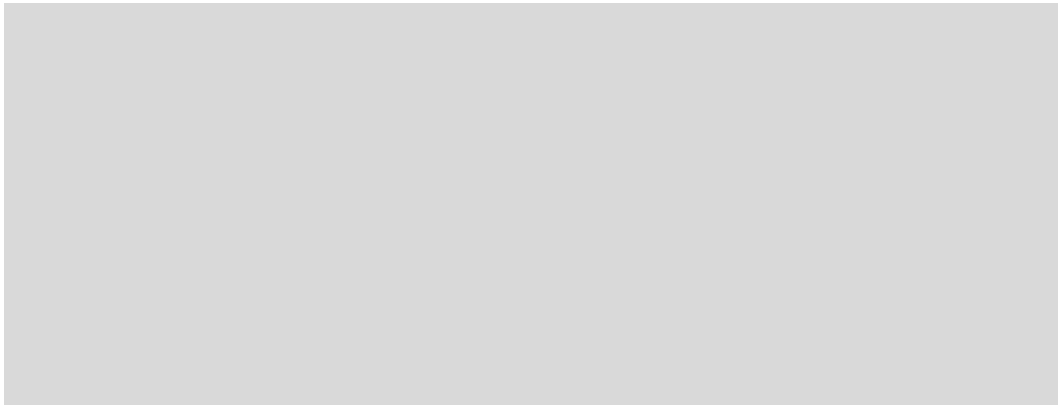


Figure S11. Triboelectric output properties of E-TENG (pair with wood): a) open-circuit voltage, b) short-circuit current.



Figure S12. 3D printed items: a) butterfly, b) shell, and c) a square surface with pyramid structures.

Supplementary Movie



Movie S1. Touch sensing applications of the E-TENG: a flexible touch switch for the protection of cultural relics.